



Lasers in Manufacturing Conference 2021

Laser melt injection for homogenous particle distribution in copper materials

Anika Langebeck^{a,*}, Annika Bohlen^a, Thomas Seefeld^a

^aBIAS – Bremer Institut fuer angewandte Strahltechnik GmbH, Klagenfurter Strasse 5, 28359 Bremen, Germany

Abstract

MMC (metal matrix composite) layers have great potential to improve abrasive wear resistance of tool surfaces such as injection molds. For this, laser melt injection is used to disperse hard particles into the molten tool surfaces. By varying the process parameters a non-homogenous particle distribution can occur. This paper addresses the systematic study to evaluate the influence of the process velocity and the powder feed rate on the particle distribution of spherical fused tungsten carbide in aluminum bronze. It is shown, that with increasing powder feed rate and decreasing process velocity a homogenous particle distribution can be achieved. The process velocity is identified as a major affecting parameter on the particle distribution. For the analyzed MMC system a process velocity of 300 mm/min led to a homogenous distribution whereas faster process velocities of 500 mm/min resulted in a graded particle distribution.

Keywords: laser melt injection; MMC; aluminum bronze; spherical fused tungsten carbide

1. Introduction

Metal matrix composites (MMC) have great potential to reduce abrasive wear in many industrial cases such as bearings, valves, and injection molding tools by improving the wear resistance (Bhattacharjee et al., 2014). MMC surfaces can be manufactured via laser melt injection (LMI) (Cabeza et al., 2014). As hard particles for reinforcement titanium, vanadium, chromium, and tungsten carbides are typically used. The latter one with an angular or spherical morphology (Nurminen et al., 2009). As matrix material ferrous and non-ferrous materials such as Ti-, Al-, Ni- and Cu-based alloys are used (Kainer, 2010). The improvement of the wear resistance by hard particle reinforcement depends on the combination of matrix material and

* Corresponding author. Tel.: +49-421-218-58035; fax: +49-421-218-58063 .
E-mail address: langebeck@bias.de .

reinforcement material (Nurminen et al., 2009). A significant increase in wear resistance can be obtained e. g. by manufacturing an MMC surface in Cu-based aluminum bronze reinforced with spherical fused tungsten carbide particles. By reinforcing the matrix material, the abrasive wear can be decreased to a quarter (Freiße et al., 2016). With increasing hard particle content, the abrasive wear resistance increases (van Acker et al., 2005). In some cases, the LMI parameters could lead to a non-homogenous particle distribution (Pei et al., 2002). This could be disadvantageous if a high hard particle content in the finished surface is the aim of the LMI process. Therefore, this paper addresses the influence of LMI parameters on the particle distribution for industrial interesting MMCs in aluminum bronze reinforced with spherical fused tungsten carbide.

2. Experimental

2.1. Materials

As reinforcing particles spherical fused tungsten carbide with a particle size of 45 μm to 106 μm and a density of 16 g/cm^3 to 17 g/cm^3 was used. As matrix material cuboid milled aluminum bronze (CuAl10Ni5Fe4) with 50 mm length, 20 mm width and 12 mm height was used. The used aluminum bronze has a density of 7.6 g/cm^3 and is a typical alloy for highly strained bearings, wearing plates and components in injection molding tools.

2.2. Set-up

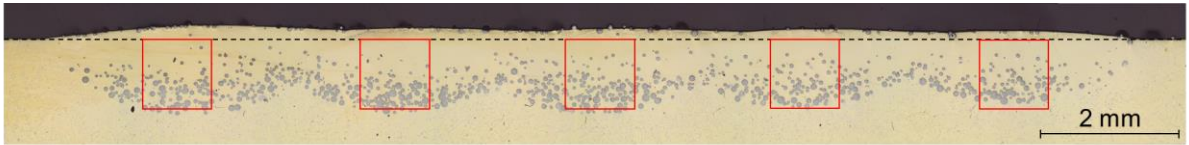
For the LMI process a Trumpf TruDisk 12002 Yb:YAG disk laser with 1030 nm wavelength and a maximum output power of 12 kW was used. The beam is guided to the processing unit via a laser light cable with 200 μm core diameter. The processing head consists of an angular Trumpf BEO D70 optical unit with 200 mm collimation length and 250 mm focal length which results in a minimum laser spot diameter of 250 μm . As traversing unit, a 3-axis CNC was used. The tungsten carbide powder was guided from a Oerlikon Metco Twin 150 rotating disk powder feeder to the discrete coaxial GTV PN6625 six-jet-nozzle with a working distance of 25 mm. As carrier and shielding gas argon was used with a flow rate of 3.5 l/min and 17 l/min, respectively.

2.3. Procedure

The effect of the LMI parameters on the particle distribution in aluminum bronze was studied on small MMC layers which were manufactured by five single tracks with a small lateral overlap. To examine the influence of the process velocity (300 mm/min, 400 mm/min and 500 mm/min) and the powder feed rate (10.7 g/mm, 15.9 g/mm and 22.3 g/mm) on the particle distribution both parameters were varied while the others were kept constant. The laser spot diameter was set to 3 mm. Depending on the set process velocity the laser power was adjusted to maintain a constant energy input per unit length of 0.24 J/m. For each parameter set two MMC-layers out of five single tracks were manufactured.

The particle distribution was studied on non-etched cross sections. Therefore, wire cut EDM was used, and the cross sections were grinded and polished. Along the cross section five regions of interest (ROIs) with the size of 1 mm width and 1 mm depth were set for each reinforced layer (see Fig. 1). For industrial applications of MMC surfaces on already existing components, it is advantageous that no prior allowance is required before LMI. Therefore, especially the particle distribution from the initial surface and below is of

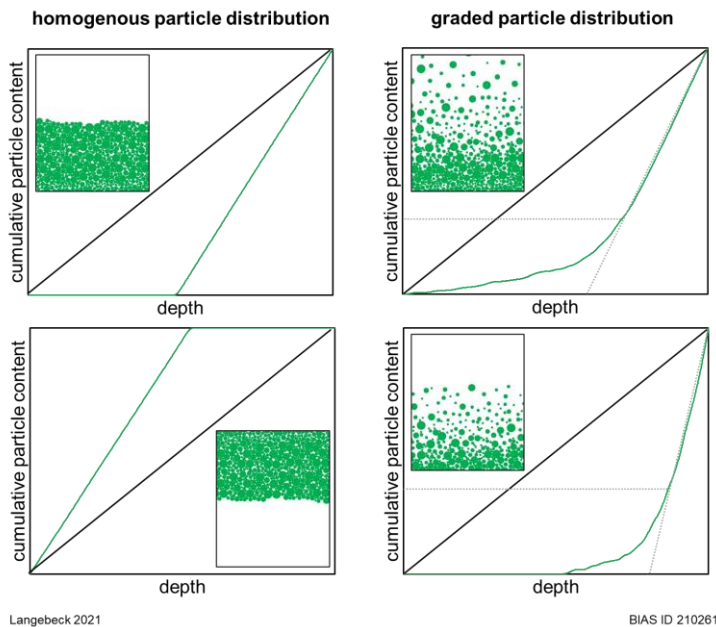
interest. That is why the top of the ROIs aligns with the initial surface of the specimen. The ROIs were recorded with a light microscope made by Zeiss at 50x magnification.



Langebeck 2021

BIAS ID 210260

Fig.1. Cross section of a MMC layer with ROI for evaluating the particle distribution



Langebeck 2021

BIAS ID 210261

Fig.2. Schematic diagrams for different particle distributions (green) deviating from an ideal homogenous distribution (black)

For a homogenous but sedimented distribution (top left) the curve resembles a straight line but has a delayed increase with a larger slope. For a homogenous distribution with a smaller melt pool than the ROI (bottom left) the curve resembles a straight line but has a larger slope. If the particle distribution is partially graded (top right) the curve can be divided into a non-linear section which indicates a graded particle distribution and a linear section which indicates a homogenous particle distribution. The dotted gray lines mark this transition between the two sections and defines the corresponding intercept at the ordinate. A high value of the cumulative particle content at this intercept describes a large area of the graded particle distribution. The bottom right diagram in Fig. 2 shows a sedimented and graded particle distribution. The corresponding curve shows a delayed increase like in the top left in Fig. 2 followed by a non-linear and a linear section like in the top right in Fig. 2.

Automated image processing was used to analyze the hard particle distribution within the ROIs by filtering and binarizing the images (for details see Freiße et al., 2019). For each pixel row the particle content was measured and cumulated to the previous ones to generate a curve of the cumulative particle content plotted against the depth of the MMC layer. For an ideal homogenous particle distribution over the whole ROI, the curve is a straight line like the black curves in Fig. 2. Depending on the particle distribution the real curves deviate from the straight line. Fig. 2 shows some examples of possible particle distributions and their corresponding curves for the cumulative particle content. For a homogenous but sedimented distribution (top left) the curve resembles a straight line but has a delayed increase with a larger

3. Results

Fig. 3 shows the cumulative particle content of the different MMC layers plotted against the depth. The red curves describe the particle distribution within the ROIs of MMC layers which were manufactured with a low powder feed rate of (10.7 ± 0.3) g/min. The blue and orange curves describe the particle distribution in the ROIs of the MMC layers which were manufactured with a higher powder feed rate of (15.9 ± 0.3) g/min and (22.3 ± 0.3) g/min, respectively. For each powder feed rate two different process velocities were used. In Fig. 3 the continuous curves show the particle distribution in MMC layers which were manufactured at 400 mm/min. The results for MMC layers manufactured at 500 mm/min are shown as dashed curves. Below the curves in Fig. 3 the corresponding cross sections are shown. When looking at these cross sections an undulating contour can be seen at the bottom edge of the MMC layers. This is due to the small lateral overlap between the MMC single tracks during the LMI process of MMC layers. The undulating contour is also visible at the upper edge of the specimens, in boundary to the black mounting resin. This topology is particularly prominent for higher powder feed rates of (15.9 ± 0.3) g/min (Fig. 3, blue) and (22.3 ± 0.3) g/min (Fig. 3, orange). Above all MMC layers a hard particle free zone can be detected. This sedimentation is due to the higher density of the spherical fused tungsten carbide particles (16 g/cm^3 to 17 g/cm^3) compared to the aluminum bronze matrix (7.6 g/cm^3). For highest powder feed rate of (22.3 ± 0.3) g/min and a low process velocity of 400 mm/min (Fig. 3, continuous orange frame) this particle free zone was above the initial surface (see dashed black line in Fig. 3, cross section with continuous orange frame). For a lower powder feed rate of (15.9 ± 0.3) g/min at the same process velocity (Fig. 3, continuous blue frame) the change between aluminum bronze with and without hard particles is in the area of the initial surface. Therefore, for both parameter sets, there is already a high hard particle content at the beginning of the ROIs. In this case the corresponding curves of the cumulative particle content (Fig. 3, continuous blue and orange curves) show no delayed increase and resemble a straight line

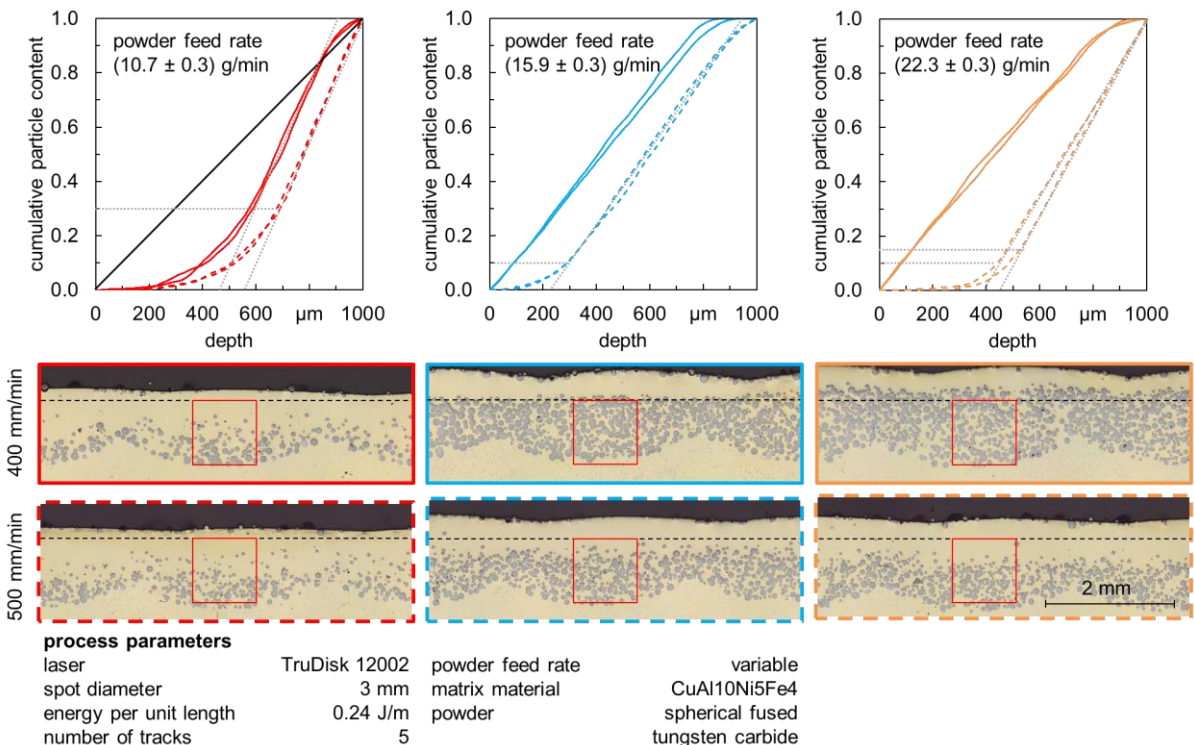


Fig. 3. Cumulative particle content plotted against depth of MMC-layers depending on the used process velocity of 400 mm/min (continuous lines) and 500 mm/min (dashed lines) for powder feed rates of (10.7 ± 0.3) g/min (red), $15.9 \pm 0.3)$ g/min (blue) and (22.3 ± 0.3) g/min (orange) as well as the corresponding cross sections of MMC layers

for an ideal homogenous particle distribution within the ROI. For all other specimens, the hard particle free zone is larger, and the ROIs covered the reinforced part and a part of this particle free zone. Therefore, the increase of the corresponding curves in Fig. 3 is delayed. Besides the delayed increase these curves show a non-linear increase at the beginning, which indicates a non-homogenous particle distribution (see Fig. 2, bottom left). The transition from the non-linear section to the linear section can be detected for the MMC layers in Fig. 3 at different cumulative particle contents (see Fig. 3, dotted gray lines). For a low powder feed rate of (10.7 ± 0.3) g/min this transition was at 30 % of the cumulative particle content regardless of the used process velocity (Fig. 3, red curves). For higher powder feed rates at a high process velocity this transition can be detected at about 10 % to 15 % of the cumulative particle content (Fig. 3, dashed blue and orange curves). This indicates a larger area with a graded particle distribution for a low powder feed rate of (10.7 ± 0.3) g/min (Fig. 3, red curves) than for higher powder feed rates (Fig. 3, dashed blue and orange curves).

For high powder feed rates of (15.9 ± 0.3) g/min and (22.3 ± 0.3) g/min the process velocity affected the particle distribution (Fig. 3, blue and orange curves), whereas for a low powder feed rate of (10.7 ± 0.3) g/min no influence of the process velocity on the homogeneity was detected (Fig. 3, red curves). For higher powder feed rates a high process velocity of 500 mm/min led to a graded particle distribution (Fig. 3, dashed blue and orange curves) and a lower process velocity of 400 mm/min led to a homogenous particle distribution within the ROIs (Fig. 3, continuous blue and orange curves). Both, powder feed rate and process velocity, affect the particle distribution.

In general, the presented results indicate that a homogenous particle distribution in MMCs in aluminum bronze reinforced with spherical fused tungsten carbide can be manufactured at lower process velocities of 400 mm/min. Nevertheless, for low powder feed rates of (10.7 ± 0.3) g/min a process velocity of 400 mm/min still led to a graded particle distribution. Further investigations showed that with a lower process velocity of 300 mm/min a homogenous particle distribution can be achieved for low powder feed rates of (10.7 ± 0.3) g/min, too (see Fig. 4). In Fig. 4 the cumulative particle content for MMC layers manufactured with lowest powder feed rate and different process velocities is shown. Additionally, exemplarily corresponding cross sections are displayed. For lowest process velocity the dash-dotted red curve shows an approximately straight line which indicates a homogenous particle distribution. This matches with the corresponding cross section. Like mentioned before higher process velocities in combination with a low powder feed rate led to a graded particle distribution.

process parameters

| | | | |
|------------------------|---------------------------|------------------|----------------------------------|
| laser | TruDisk 12002 | powder feed rate | (10.7 ± 0.3) g/min |
| spot diameter | 3 mm | matrix material | CuAl10Ni5Fe4 |
| energy per unit length | 0.24 J/mm | powder | spherical fused tungsten carbide |
| | 0.26 J/mm (at 300 mm/min) | | |
| number of tracks | 5 | | |

| | process velocity | | |
|------------------------|------------------|------------|------------|
| | 300 mm/min | 400 mm/min | 500 mm/min |
| (10.7 ± 0.3) g/min | 0.036 g/mm | 0.027 g/mm | 0.021 g/mm |

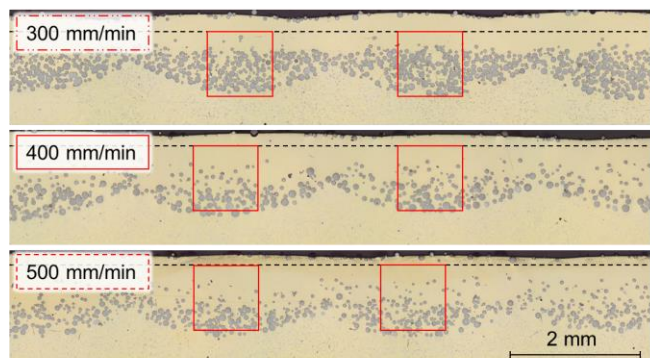
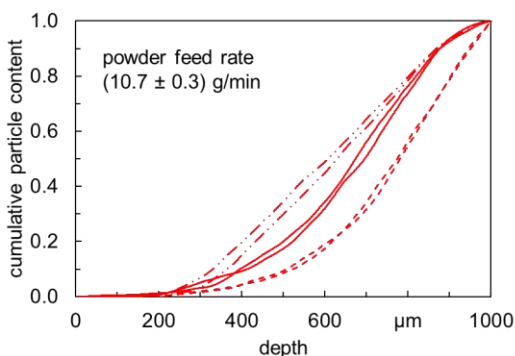
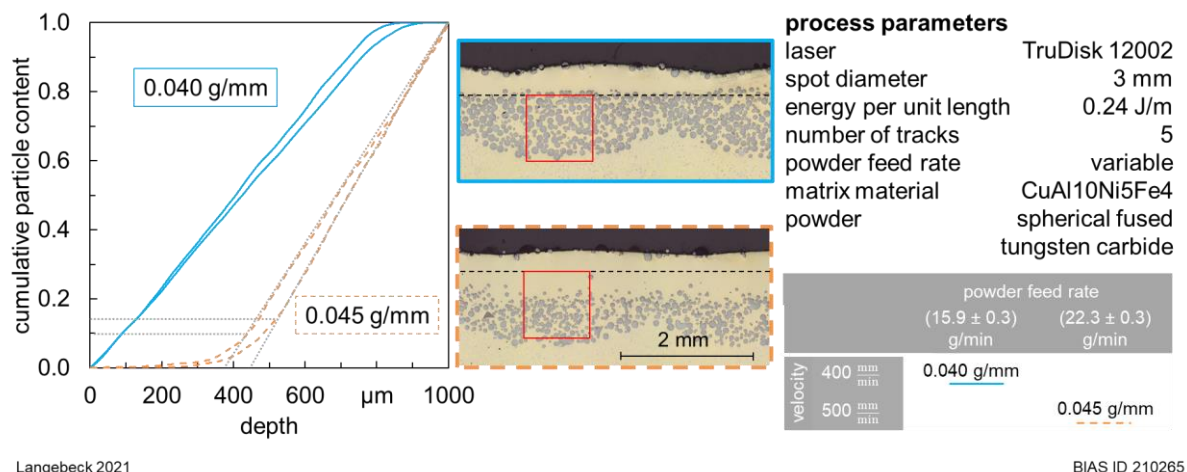


Fig. 4. Cumulative particle content plotted against depth of MMC layers depending on the used process velocity for a powder feed rate of (10.7 ± 0.3) g/min and cross sections of these MMC layers

4. Discussion

Both the powder feed rate and the process velocity showed an effect on the particle distribution. With increasing powder feed rate and decreasing process velocity homogenous particle distributions were detected. These direct LMI parameters can be combined to the indirect parameter powder feed rate per unit length, the quotient of powder feed rate and process velocity. This indirect parameter can be increased either by increasing the powder feed rate or decreasing the process velocity. Both cases of parameter variation led to a more homogenous particle distribution (Fig. 3). Therefore, it could be suggested, that rather this indirect parameter affects the particle distribution and less the direct process parameters powder feed rate and process velocity. Fig. 5 shows the cumulative particle content and exemplarily corresponding cross sections of MMC layers which were manufactured with a comparable powder feed rate per unit length of 0.040 g/mm (continuous blue curve) and 0.045 g/mm (dashed orange curve). It can be found that, despite comparable powder feed rates per unit length, different particle distributions were measured. The blue curves describe a homogenous particle distribution in the ROIs of MMC layers manufactured with a powder feed rate of (15.9 ± 0.3) g/min at a process velocity of 400 mm/min. Whereas the orange curves in Fig. 5 describe slightly graded particle distribution in the ROIs of MMC layers manufactured with a higher powder feed rate of (22.3 ± 0.3) g/min at a higher process velocity of 500 mm/min. Fig. 5 show, that a graded particle distribution occurs only for the slightly higher powder feed rate per unit length of 0.045 g/mm (Fig. 5, dashed orange curve). This is contradictory to the assumption, that a higher powder feed rate per unit length would result in a homogenous particle distribution. The data indicates that the influence of a high process velocity for a graded particle distribution superimposes that of a high powder feed rate for a homogenous particle distribution (see Fig. 5, dashed orange curves). Thus, the process velocity can be identified as a major influencing factor on the particle distribution in MMC layers produced by LMI. By further decreasing the process velocity for low powder feed rates of (10.7 ± 0.3) g/min this assumption can be validated. Since a process velocity of 300 mm/min led to a homogenous particle distribution. The influence of the process velocity on the particle distribution can be explained by the solidification of the melt pool. During the solidification the viscosity of the melt pool increases until the melt pool is completely solidified. As a result, particles entering the melt pool at a later stage penetrate the melt pool less deeply due to the increased viscosity, and grading occurs (Pei et al., 2002). With increasing process velocity at constant energy input per unit length, the solidification of the melt pool accelerates. Thus, a graded particle distribution is formed at higher process velocities.



Langebeck 2021

BIAS ID 210265

Fig. 5. Cross sections and cumulative particle content plotted against depth of MMC layers for comparable powder feed rate per unit length but different process velocity and powder feed rate

5. Conclusion

The particle distribution in MMCs is affected by the powder feed rate as well as the process velocity. With increasing powder feed rate and decreasing process velocity homogenous particle distributions can be achieved. The process velocity has a major impact on the homogeneity. For the studied MMC system aluminum bronze reinforced with spherical fused tungsten carbide low process velocities of 300 mm/min led to a homogenous particle distribution for the studied cases.

Acknowledgements

The IGF-Project with the IGF-No.: 19.941 N / DVS-No.: 06.3046 of the "Forschungsvereinigung Schweißen und verwandte Verfahren e. V." of the German Welding Society (DVS), Aachener Str. 172, 40223 Düsseldorf was funded by the Federal Ministry for Economic Affairs and Energy (BMWi) via the German Federation of Industrial Research Associations (AiF) in accordance with the policy to support the Industrial Collective Research (IGF) on the basis of a decision by the German Bundestag. Furthermore, the authors gratefully acknowledge the collaboration with the members of the project affiliated committee regarding the support of knowledge, material and equipment over the course of the research.

The "BIAS ID" nos. are part of the figures and allow the retraceability of the results with respect to mandatory documentation required by the funding organization.

Supported by:



on the basis of a decision
by the German Bundestag



References

- Bhattacharjee, D., Muthusamy, K., Ramanujam, S., 2014. Effect of Load and Composition on Friction and Dry Sliding Wear Behavior of Tungsten Carbide Particle-Reinforced Iron Composites. *Tribology Transactions* 57, 292–299.
- Cabeza, M., Castro, G., Merino, P., Pena, G., Roman, M., 2014. A study of laser melt injection of TiN particles to repair maraging tool steels. *Surface and Interface Analysis* 46, 861–864.
- Freiße, H., Bohlen, A., Seefeld, T., 2019. Determination of the particle content in laser melt injected tracks. *Journal of Materials Processing Technology* 267, 177–185.
- Freiße, H., Vollertsen, F., Langebeck, A., Köhler, H., Seefeld, T., 2016. Dry strip drawing test on tool surfaces reinforced by hard particles. *Dry Metal Forming Open Access Journal* 2, 1–6.
- Kainer, K.U., 2010. *Metal matrix composites: Custom-made materials for automotive and aerospace engineering*. Weinheim, Chichester: Wiley-VCH.
- Nurminen, J., Näkki, J., Vuoristo, P., 2009. Microstructure and properties of hard and wear resistant MMC coatings deposited by laser cladding. *International Journal of Refractory Metals and Hard Materials* 27, 472–478.
- Pei, Y.T., Ocelik, V., Hosson, J.T.M. de, 2002. SiCp/Ti6Al4V functionally graded materials produced by laser melt injection. *Acta Materialia* 50, 2035–2051.
- van Acker, K., Vanhoyweghen, D., Persoons, R., Vangrunderbeek, J., 2005. Influence of tungsten carbide particle size and distribution on the wear resistance of laser clad WC/Ni coatings. *Wear* 258, 194–202.